Vibronic Coupling in the Valence Band Photoemission of the Ferroelectric Copolymer: Poly(vinylidene fluoride) (70%) and Trifluoroethylene (30%)

Luis G. Rosa,[†] Ya. B. Losovyj,[†,‡] Jaewu Choi,[†,§] and P. A. Dowben*[,†]

Department of Physics and Astronomy and the Center for Materials Research and Analysis, Behlen Laboratory of Physics, University of Nebraska−Lincoln, Lincoln, Nebraska 68588-0111, Center for Advanced Microstructures and Devices, Louisiana State University, 6980 Jefferson Highway, Baton Rouge, Louisiana 70806, and Department of Electrical and Computer Engineering, Wayne State University, 5050 Anthony Wayne Drive #3100, Detroit, Michigan 48202

Received: December 13, 2004; In Final Form: February 17, 2005

Two different vibrational contributions to the photoemission fine structure of the ferroelectric copolymer poly(vinlylidene fluoride) with trifluoroethylene (CH_2-CF_2:$CHF-CF_2$, 70%:30%) are identified. The vibrational contributions at the higher photoemission binding energies are associated with two closely placed $\upsilon_{a,s}$ (CH_2) stretching modes while at the smaller photoemission binding energies, the fine structure is due to a δ (CH_2) bending mode. The contribution of the δ (CH_2) mode to the photoemission fine structure decreases with decreasing temperature. We associate this temperature dependence to the importance of symmetry in vibronic coupling to the photoemission process and increased dipole ordering with decreasing temperature in this organic ferroelectric system.

1. Introduction

The existence of contributions of the vibrational modes to the photoemission spectra of the molecular orbitals of gas phase[1,2] and adsorbed[3] molecules have long been recognized. For larger molecules, the vibronic fine structure in the photoemission or photoionization spectra of molecules can be quite complex[4,5] and can often defy identification even in gas-phase molecular systems.[6] There are some notable exceptions such as in the photoemission spectra of ferrocene[7] and adsorbed metal phthalocyanines,[8] where the vibronic fine structure in the valence band photoemission compares well with the infrared and high-resolution electron energy loss spectra in refs 9 and 10, respectively.

Polymers based on the simple alkane, alkene, and alkyne chains, even when fluorinated, should have fairly simple vibronic fine structure contributions to the photoemission spectra, based upon the existing studies of the small alkanes,[11] including the core level spectra[12] and studies of adsorbed species.[13] Because the vibrational modes must share symmetry and couple to the ionized final state of the molecule to provide the necessary photoemission fine structure, high-resolution photoemission is a means to indirectly probe electron−phonon coupling in molecular systems.

The ferroelectric copolymer poly(vinlylidene fluoride) with trifluoroethylene (CH_2-CF_2:$CHF-CF_2$, 70%:30%), P(VDF−TrFE), is a well-known ferroelectric system,[14,15] which can exhibit exceptional surface order when prepared ex situ by Langmuir−Blodgett monolayer deposition from a water subphase and then annealed in a vacuum.[16−20] Photoemission[21−27] and high-resolution electron energy loss[24,26−28] spectroscopy studies have been undertaken on the crystalline surfaces of copolymer films of polyvinylidene fluoride with 30% of trifluoroethylene, P(VDF−TrFE 70:30). The experimental band structure[16,17] and band symmetries[26] of the crystalline polymer have been successfully compared to theory.[29]

Of interest are the various phase transitions such as a surface phase transition at about 295 K[16,17,22,26] and a compressibility (lattice stiffening) at about 160 K[24,27,28] (distinct from the bulk ferroelectric transition at about 350 K) where electron−phonon coupling has been implicated.[21,24] While dipole ordering is expected for the ferroelectric transition, other possible types of dipole ordering may play a role in the various phase transitions exhibited by this system[21,24] and are directly explored here.

2. Experimental and Theoretical Details

The very thin crystalline poly(vinylidene-fluoride with trifluoroethylene: 70%:30%), P(VDF−TrFE 70:30), films were formed by Langmuir−Blodgett monolayer deposition from water subphase, as described elsewhere.[14,15] The films were prepared by gentle annealing to 150 °C in vacuo and have been shown to be electronically similar to films prepared in situ.[27] Throughout this work, we used nominally 6 monolayer films on graphite for the high-resolution ultra violet photoemission (UPS) experiments, and 2 monolayer films of P(VDF−TrFE 70:30) on heavily doped silicon, for the electron energy loss spectroscopy (EELS) measurements. The high-resolution electron energy loss spectroscopy (HREELS) was undertaken using a LK-2000 spectrometer at Oak Ridge National Laboratory. The high-resolution ultra violet photoemission spectroscopy (UPS) was done using a helium lamp at $h\nu = 21.2$ eV (He I) and a Scienta 200 hemispherical electron analyzer and by collecting the photoelectrons emitted normal to the surface normal. The combined resolution was better than 10 meV, as inferred from widths of the photoionization spectra for the Ar $3p_{1/2}$ (15.9 eV) and $3p_{3/2}$ (15.7 eV), shown in Figure 1. All binding energies are referenced with respect to the Fermi edge of gold, measured at 80 K, which exhibited a thermal spreading of about 30 meV consistent with this temperature.

* Corresponding author. Phone: (402) 472-9838. Fax: (402) 472-2879. E-mail: pdowben@unl.edu.
[†] University of Nebraska−Lincoln.
[‡] Louisiana State University.
[§] Wayne State University.

10.1021/jp044323j CCC: $30.25
Published on Web 03/24/2005

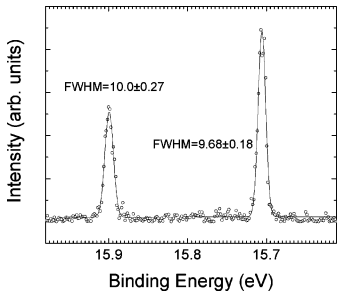

Figure 1. High-resolution photoemission spectra for the Ar 3p state showing the widths of the peaks to be about 9−10 meV.

The light polarization photoemission spectra were taken at 42 eV photon energy using light from a plane grating monochromator at the Center for Advanced Microstructures and Devices. Again, the electrons were collected along the surface normal but the combined resolution of the beamline and electron energy analyzer was about 200 meV, as described elsewhere.[26,27]

The vibrational modes determined from high-resolution electron energy loss and high-resolution photoemission are compared to semiempirical calculations for a molecule of 4 monomers of vinylidene fluoride and 2 monomers of trifluoroethylene for both the all-trans configuration and the alternating gauche and trans configuration structures. The vibrational modes were calculated with an MNDO-PM3 (modified neglect of differential overlap, parametric method 3) and Hamiltonian. This Hamiltonian does not include solid-state effects and dipole−dipole coupling. These semiempirical model calculations of the electronic structure were performed following geometry optimization (C_{2v} for the all-trans configuration and C_s for the alternating gauche and trans configuration), and the vibrational modes were then calculated. The optimized geometrical parameters in these calculations are as follows: the bond lengths of C−C, C−F, and C−H are 1.568, 1.380, and 1.087 Å, respectively. The dihedral angles of C−C_F−C, C_F−C−C_F, H−C−H, F−C−F, C−C−F, and C−C−H are 110.3°, 112.5°, 108.6°, 107.3°, 109.9°, and 108.9°, respectively, where the subscript F indicates a carbon atom that is bonded with a fluorine atom(s).

The vibrational modes obtained from the semiempirical calculation were compared to the ab initio calculation derived from the Gaussian method with the STO-3G basis set, in a fashion similar to that undertaken for adsorbed molecules elsewhere.[9,27] The latter ab initio calculations show a larger deviation from experiment, so we restrict the discussion here to a comparison with the semiempirical calculations.

3. Evidence of Vibrational Fine Structure on the Photoemission Spectra of P(VDF−TrFE: 70%, 30%)

The high-resolution photoemission spectra taken here with unpolarized He I radiation differ somewhat from photoemission spectra taken with light incident angle-dependent polarized light (i.e., synchrotron radiation as in refs 26,27). With polarized light, one can identify strong bands appearing at the binding energies of 8.2 eV (B_1,B_2), 10.9 eV (B_1,B_2), 11.8 eV (A_1), 12. 5 eV, 14.9 eV (B_1,B_2), and 16.5 eV (A_1) as seen in the inset to Figure 2a. Some of these same features can be identified in the photoemission spectra with unpolarized light but with a somewhat different distribution of intensity contributions from the features with strong B_1,B_2 molecular orbital character than is observed in the spectra taken with linearly polarized light.

Fine structure in the photoemission spectra is evident in these high-resolution photoemission spectra shown in Figure 2b. This fine structure corresponds to the excitation of two vibrational modes. The first mode between 11.5 and 14 eV binding energy

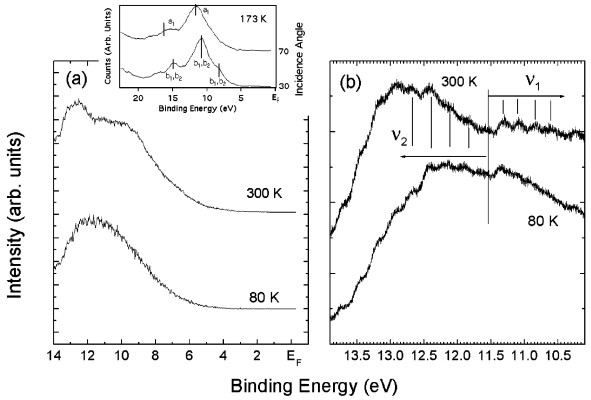

Figure 2. Valence band photoemission spectra taken at normal emission as a function of temperature from (a) nominally 5 monolayer crystalline films of P(VDF−TrFE 70:30) fabricated ex situ by Langmuir−Blodgett techniques. In (b), the region with the vibronic fine structure is enhanced, with the vibrational contributions indicated (see text). The incident photon energy is 21.2 eV. The inset shown the light polarization photoemission spectra taken at a photon energy of 42 eV. In the inset, the 30° light incidence angle indicates more s polarized light, while the 70° light incidence indicates more p-polarized light. The band symmetries are indicated in the inset.

in Figure 2b corresponds to about 2400 cm^{-1} (the ν_2 mode at about 300 meV), and the second vibrational mode evident in the photoemission spectra between 10 and 11.5 eV binding energy has a frequency of 1890 cm^{-1} (the ν_1 mode at about 230 meV). While one generally ascribes the vibrational coupling to the photoemission process as a Franck−Condon transition, these vibrational modes observed in the high-resolution photoemission at 2400 and 1890 cm^{-1} can only be a result of the excitation of various CH_2 related modes. As seen in Table 1, there are two υ_a (CH_2) modes near 3000 cm^{-1} and a strong δ (CH_2) mode near 1600 cm^{-1}. These two modes observed in the high-resolution photoemission spectra are only a few of the known modes.

In fact, six vibrational bands of PVDF−TrFE thin films, as summarized in Table 1, can be identified in the high-resolution electron energy loss (HREELS) data (Figure 3a), which are largely in agreement with the semiempirical calculations.[26] The vibrational dipole active modes at 450 cm^{-1} (CF_2 bending modes) and 900 cm^{-1} (CF_2 and CH_2 rocking modes) are strongly active below the surface ferroelectric phase transition at 290−300 K. The dipole active mode at 1150 cm^{-1} (the CF_2 stretch modes and CH_2 rocking modes) seems to endure through the surface and bulk phase transitions at 300 and 355 K, respectively. The 1360 cm^{-1} (CH_2 wagging and CC stretch mode), 1580 cm^{-1} (CH_2 bending mode), and 2900 cm^{-1} (CH_2 stretch mode) are not dipole active modes, but observed nonetheless. The calculated frequencies reported here tend to be somewhat higher than those measured and calculated by K. Tashiro and co-workers,[30] but otherwise are in good general agreement with prior work.[26]

Our free molecule calculations, using semiempirical models, show that the formation of a positive ion in the polymer chain results in a shift in the vibrational modes energy lower values, by about 500 cm^{-1}. This correction to the calculated vibrational modes applies to the fine structure in the photoemission spectra as a result of the photohole left in the photoemission process (hole vibrational coupling as in possible dipole mode excitations observed in the high-resolution photoemission of the metal phthalocyanines[8]). Taking into account this shift in the vibrational mode energy allows us to assign the vibrational "ν_2 mode" observed in high-resolution photoemission of PVDF−TrFE at 2400 cm^{-1} to the two $\upsilon_{a,s}$ (CH_2) modes near 3000 cm^{-1}

TABLE 1: Comparison of Calculated Vibrational Modes of All-Trans Geometric Structure for Both PVDF and P(VDF−TrFE) with High-Resolution Electron Energy Loss Spectroscopy[26] and the Work of Tashiro et al.[30]

vibrational properties		PVDF (cm^{-1})			P(VDF−TrFE) (cm^{-1})	
modes[a]	symmetry representation	MO theory	EELS	ref[30]	MO theory	EELS
υ_a (CH_2)	B_2	3052	2995 ± 82	3021	3044	2922 ± 74
υ_s (CH_2)	A_1	2985		2993	2982	
δ (CH_2)	A_1	1560	1650 ± 82	1429	1547	1580 ± 74
υ_a (CC)	B_1	1552		1389	1542	
w(CH_2)	B_1	1504		1389	1539	
υ_s (CF_2)	A_1	1496	1382 ± 100	1270	1494	1360 ± 100
υ_s (CC)	A_1	1487		1270	1469	
δ (CCC)	A_1	1477		1270	1467	
υ_a (CF_2)	B_2	1317		1180	1340	
r(CH_2)	B_2	1316	1177 ± 100	1180	1322	1166 ± 100
υ_a (CC)	B_1	1306		1063	1240	
t (CH_2)	A_2	1067		953	1095	
υ_a (CF_2)	B_2	1028		897	1040	
r(CH_2)	B_2	965		897	1001	
r(CF_2)	B_2	948	914 ± 82	897	984	892 ± 74
υ_s (CF_2)	A_1	948		837	966	
υ_s (CC)	A_1	785		837	937	
δ (CF_2)	A_1	540	524 ± 82	504	639	526 ± 74
w (CF_2)	B_1	528		470	560	
r (CF_2)	B_2	468		430	507	
t (CF_2)	A_2	243		255	258	

[a] The vibrational modes are identified by $\upsilon_{s,a}$ for symmetric or antisymmetric stretching modes, δ for bending modes, w for wagging mode, r for rocking mode, and t for twisting modes and by symmetry (assuming a C_{2v} point group symmetry).

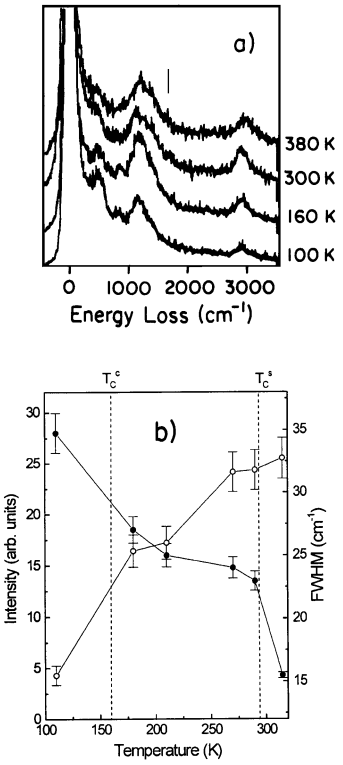

Figure 3. Electron energy loss spectra (a) taken at the specular geometry (dipole active), as a function of temperature, from a 2 monolayer P(VDF−TrFE 70:30) film formed by Langmuir−Blodgett techniques. The intensity of the 450 cm^{-1} dipole active mode (○) and the width of the 1150 cm^{-1} dipole active mode (●), abstracted from the HREELS data are plotted as a function of temperature (b) and with the lattice stiffening transition T_C^c at about 160 K[19,22,23] and the surface ferroelectric transition T_C^s at 290−310 K[11,12,17,21] indicated.

predicted by theory (summarized in Table 1) and observed in high-resolution electron energy loss spectroscopy shown in Figure 3a. This assignment is consistent with studies of the chloromethanes[31] that found very little vibrational fine structure contribution to the photoemission spectra from C−H bending modes and greater contributions from υ_a-like modes.

It is more difficult to assign the "ν_1 mode" at 1890 cm^{-1} (about 230 meV) contributing to the fine structure in the photoemission spectra at lower photoemission binding energies. The decrease in intensity of this fine structure, in the photoemission spectra, with decreasing temperature, allows us to assign this vibrational mode to a δ (CH_2) mode near 1600 cm^{-1}, as discussed below. The fact that this mode appears at much higher energy than the corresponding mode in our model calculations (Table 1) and observed high-resolution electron energy loss (Figure 3a) can only be attributed to solid-state effects. This is a bending mode that could easily be made stiffer through dipole−dipole extra molecular interactions. The stiffening of this mode by solid-state effects is suggested by our experimental high-resolution electron energy loss spectra: this is one of the few modes observed in experiment at a higher energy than predicted by theory (see Table 1). Such extra molecular interactions leading to this effect could be enhanced by the photohole left in the photoemission process. Extra molecular effects may also influence the vibronic fine structure observed in the photoemission of the metal phthalocyanines.[8]

4. Suppression of Vibrational Modes Due to Dipole Ordering

Dipole ordering is evident from the HREELS data presented in Figure 3. The vibrational dipole active modes at 450 cm^{-1} (CF_2 bending modes) and 900 cm^{-1} (CF_2 and CH_2 rocking modes) are strongly active below the surface ferroelectric phase transition at 290−300 K, while increasing in intensity even further at temperatures below the compressibility phase transition at 160 K. This is fully consistent with increasing dipole alignment along the surface normal with decreasing temperatures, particularly at the surface phase transition at about 295 K[16,17,22,26] and a compressibility (lattice stiffening) at about 160 K.[24,27,28]

The δ (CH_2) mode near 1600 cm^{-1} is not a strong dipole active mode, as can be inferred from the high-resolution electron energy loss data,[26] but it is nonetheless of A_1 symmetry. As the dipole ordering becomes increasingly better defined with decreasing temperature, the symmetry restrictions on the photoemission bands as well as the vibrational modes become more

rigid. In other words, the symmetry assignments at higher temperatures are much less restrictive because there is canting of the dipoles, and this canting of dipoles can be significant enough to be observed in scanning tunneling microscopy.[20] If the ν_1 mode observed at about 230 meV in the high-resolution photoemission is also of A_1 symmetry, then as the temperature decreases, this mode cannot easily couple with photoemission bands of B_1,B_2 symmetry.

The pronounced decrease, with decreasing temperature, in the photoemission fine structure associated with the ν_1 mode, observed at about 230 meV in the high-resolution photoemission, is indicative of this fine structure resulting from a symmetry restricted vibrational mode of A_1. This is because the photoemission spectra are dominated by bands of B_1,B_2 symmetry at the smaller binding energies.[26] On this basis, we can only assign the ν_1 mode observed at about 230 meV, in the high-resolution photoemission, to a mode of A_1 symmetry, and the only possible choice is the δ (CH_2) mode calculated to be in the vicinity of 1600 cm^{-1}. Although this energy does not match that observed in high-resolution photoemission, as noted above, this value both calculated and observed in HREELS does not account for solid-state effects that may be enhanced in the presence of the photohole. Obviously, more sophisticated theory is needed to address this point more directly.

The fact that the "ν_2 mode" observed in the high-resolution photoemission of PVDF−TrFE at about 2400 cm^{-1} is assigned to two υ_a (CH_2) modes of A_1 and B_2 symmetry means that this vibrational contribution to the photoemission fine structure will be far less sensitive to dipole order with temperature, as is in fact observed.

5. Summary

There are two different vibrational contributions to the photoemission fine structure of the ferroelectric copolymer poly(vinlylidene fluoride) with trifluoroethylene (CH_2−CF_2:CHF−CF_2, 70%:30%). The vibrational contributions are expected to be more easily observed with decreasing temperature due to decreased width. Surprisingly, the contribution of one vibrational mode to the photoemission fine structure decreases with decreasing temperature. We associate this temperature dependence to the importance of symmetry in vibronic coupling to the photoemission process and increased dipole ordering with decreasing temperature in this ferroelectric system.

Acknowledgment. This work was supported by the National Science Foundation through grant CHE-0415421 and the NSF "QSPINS" MRSEC (DMR-0213808). We would like to acknowledge the assistance and the help of Jens Braun and E. W. Plummer with the EELS measurements at ORNL.

References and Notes

(1) Heilbronner, E.; Muszkat, K. A.; Schazublin, G. *Helv. Chim. Acta* **1971**, *54*, 58. Hollas, J. M.; Sutherley, T. A. *Mol. Phys.* **1971**, *21*, 183. Hollas, J. M.; Sutherley, T. A. *Mol. Phys.* **1971**, *22*, 213.

(2) Price, W. C. Ultraviolet Photoelectron Spectroscopy: Basic Concepts and Spectra of Small Molecules. In *Electron Spectroscopy: Theory Techniques and Applications*; Brundle, C. R., Baker, A. D., Eds.; Academic Press: New York, 1977; Vol. 1, p 151.

(3) Gadzuk, J. W. *Phys. Rev. B* **1976**, *14*, 5458. Gadzuk, J. W. *Phys. Rev. B* **1979**, *20*, 515.

(4) Ray, K.; Shanzer, A.; Waldeck, D. H.; Haaman, R. *Phys. Rev. B* **1999**, *60*, 13347.

(5) Höfer, U.; Umbach, E. *J. Electron Spectrosc. Relat. Phenom.* **1990**, *54/55*, 591.

(6) Heilbronner, E.; Maier, J. P. Some Aspects of Organic Photoelectron Spectra. In *Electron Spectroscopy: Theory Techniques and Applications*; Brundle, C. R., Baker, A. D., Eds.; Academic Press: New York, 1977; Vol. 1, p 151.

(7) Rabalais, J. W.; Werme, L. O.; Bergmark, T.; Karson, L.; Hussain, M.; Siegbahn, K. *J. Chem. Phys.* **1972**, *57*, 1185.

(8) Kera, S.; Yamane, H.; Sakuragi, I.; Okudaira, K. K.; Ueno, N. *Chem. Phys. Lett.* **2002**, *364*, 93. Yamane, H.; Honda, H.; Fukagawa, H.; Ohyama, M.; Hinuma, Y.; Kera, S.; Okudaira, K. K.; Ueno, N. *J. Electron Spectrosc. Relat. Phenom.* **2004**, *223*, 137−140.

(9) Waldfried, C.; Welipitiya, D.; Hutchings, C. W.; de Silva, H. S. V.; Gallup, G. A.; Dowben, P. A.; Pai, W. W.; Zhang, J.; Wendelken, J. F.; Boag, N. M. *J. Phys. Chem. B* **1997**, *101*, 9782−9789.

(10) Azuma, Y.; Yokota, T.; Kera, S.; Aoki, M.; Okudaira, K. K.; Harada, Y.; Ueno, N. *J. Electron Spectrosc. Relat. Phenom.* **1998**, *881*, 88−91.

(11) Wang, L.; Pollard, J. E.; Lee, Y. T.; Shirley, D. A. *J. Chem. Phys.* **1987**, *86*, 3216. Cvitas, T.; Güsten, H.; Klasinc, L. *J. Chem. Phys.* **1979**, *70*, 57. Somasundram, K.; Hardy, N. C. *J. Chem. Phys.* **1986**, *84*, 2899. Stockbauer, R.; Inghram, M. G. *J. Electron Spectrosc. Relat. Phenom.* **1974**, *7*, 492. Willitsch, S.; Hollenstein, U.; Merkt, F. *J. Chem. Phys.* **2004**, *120*, 1761. Pollard, J. E.; Trevor, D. J.; Reutt, J. E.; Lee, Y. T.; Shirley, D. A. *J. Chem. Phys.* **1984**, *81*, 5302. Dehmer, P. M.; Dehmer, J. L. *J. Chem. Phys.* **1979**, *70*, 4574. Branton, G. R.; Frost, D. C.; Makita, T.; McDowell, C. A.; Stenhouse, I. A. *J. Chem. Phys.* **1970**, *52*, 802. Turner, D. W.; Baker, C.; Baker, A. D.; Brundle, C. R. *Molecular Photoemission Spectroscopy*; Wiley-Interscience: New York, 1970.

(12) Bozek, J.; Carroll, T. X.; Hahne, J.; Saethre, L. J.; True; Thomas, T. D. *Phys. Rev. A* **1998**, *57*, 157. Hergenhahn, U. *J. Phys. B: At. Mol. Opt. Phys.* **2004**, *37*, R89. Rennie, E. E.; Hergenhahn, U.; Kugeler, O. *J. Chem. Phys.* **2002**, *117*, 6524−6532. Sorensen, S. L.; Wiklund, M. *Phys. Rev. A* **1998**, *58*, 1879−1884.

(13) Wiklund, M.; Jaworowski, A.; Strisland, F.; Beutler, A.; Sandell, A.; Nyholm, R.; Sorensen, S. L.; Andersen, J. N. *Surf. Sci.* **1998**, *418*, 210−218. Hirschmugl, C. J.; Paolucci, G.; Esch, F.; Lizzit, S.; Schindler, K.-M. *Surf. Sci.* **2001**, *488*, 43−51. Wiklund, M.; Beutler, A.; Nyholm, R.; Andersen, J. N. *Surf. Sci.* **2000**, *461*, 107−117. Sock, M.; Eichler, A.; Surnev, S.; Andersen, J. N.; Klötzer, B.; Hayek, K.; Ramsey, M. G.; Netzer, F. P. *Surf. Sci.* **2003**, *545*, 122−136. Ramsvik, T.; Borg, A.; Worren, T.; Kildemo, M. *Surf. Sci.* **2002**, *511*, 351−358.

(14) Blinov, L. M.; Fridkin, V. M.; Palto, S. P.; Bune, A. V.; Dowben, P. A.; Ducharme, S. *Usp. Fiz. Nauk [Russian edition]* **2000**, *170*, 247−262; *Phys. Usp. [English edition]* **2000**, *43*, 243−257.

(15) Ducharme, S.; Palto, S. P.; Fridkin, V. M. Ferroelectric Polymer Langmuir−Blodgett Films. In *Handbook of Surfaces and Interfaces of Materials, vol. 3, Ferroelectric and Dielectric Films*; 2000; Chapter 11, pp 546−592.

(16) Choi, J.; Dowben, P. A.; Ducharme, S.; Fridkin, V. M.; Palto, S. P.; Petukhova, N.; Yudin, S. G. *Phys. Lett. A* **1998**, *249*, 505−511.

(17) Choi, J.; Borca, C. N.; Dowben, P. A.; Bune, A.; Poulsen, M.; Pebley, S.; Adenwalla, S.; Ducharme, S.; Robertson, L.; Fridkin, V. M.; Palto, S. P.; Petukhova, N.; Yudin, S. G. *Phys. Rev. B* **2000**, *61*, 5760−5770.

(18) Qu, H.; Yao, W.; Garcia, T.; Zhang, J.; Sorokin, A. V.; Ducharme, S.; Dowben, P. A.; Fridkin, V. M. *Appl. Phys. Lett.* **2003**, *82*, 4322.

(19) Palto, S.; Blinov, L.; Dubovik, E.; Fridkin, V.; Petukhova, N.; Sorokin, A.; Verkovskaya, K.; Yudin, S.; Zlatkin, A. *Europhys. Lett.* **1996**, *34*, 465.

(20) Cai, L.; Qu, H.; Lu, C.; Ducharme, S.; Dowben, P. A.; Zhang, J. *Phys. Rev. B* **2004**, *70*, 155411.

(21) Borca, C. N.; Choi, J.; Adenwalla, S.; Ducharme, S.; Dowben, P. A.; Robertson, L.; Fridkin, V. M.; Palto, S. P.; Petukhova, N. *Appl. Phys. Lett.* **1999**, *74*, 347−349.

(22) Choi, J.; Dowben, P. A.; Pebley, S.; Bune, A. V.; Ducharme, S.; Fridkin, V. M.; Palto, S. P.; Petukhiva, N. *Phys. Rev. Lett.* **1998**, *80*, 1328.

(23) Choi, J.; Dowben, P. A.; Borca, C. N.; Adenwalla, S.; Bune, A. V.; Ducharme, S.; Fridkin, V. M.; Palto, S. P.; Petukhova, N. *Phys. Rev. B* **1999**, *59*, 1819−1824.

(24) Borca, C. N.; Adenwalla, S.; Choi, J.; Sprunger, P. T.; Ducharme, S.; Robertson, L.; Palto, S. P.; Liu, J.; Poulsen, M.; Fridkin, V. M.; You, H.; Dowben, P. A. *Phys. Rev. Lett.* **1999**, *83*, 4562−4565.

(25) Choi, J.; Manohara, H. M.; Morikawa, E.; Sprunger, P. T.; Dowben, P. A.; Palto, S. P. *Appl. Phys. Lett.* **2000**, *76*, 381−383.

(26) Choi, J.; Tang, S.-J.; Sprunger, P. T.; Dowben, P. A.; Fridkin, V. M.; Sorokin, A. V.; Palto, S. P.; Petukhova, N.; Yudin, S. G. *J. Phys.: Condens. Matter* **2000**, *12*, 4735−4745.

(27) Choi, J.; Morikawa, E.; Ducharme, S.; Dowben, P. A. *Chem. Phys. Lett.*, submitted.

(28) Borca, C. N.; Adenwalla, S.; Choi, J.; Robertson, L.; You, H.; Fridkin, V. M.; Palto, S. P.; Petukhova, N.; Dowben, P. A. *Appl. Surf. Sci.* **2001**, *175−176*, 265−269.

(29) Duan, C.; Mei, W. N.; Hardy, J. R.; Ducharme, S.; Choi, J.; Dowben, P. A. *Europhys. Lett.* **2003**, *61*, 81−87.

(30) Tashiro, K.; Abe, Y.; Kobayashi, M. *Ferroelectrics* **1995**, *171*, 281.

(31) Sudin, S.; Saethre, L. J.; Ausmees, A.; Svensson, S. *J. Chem. Phys.* **1999**, *110*, 5806.